ANTIMICROBIAL AGENTS AND CHEMOTHERAPY, Apr. 2010, p. 1580–1589 Vol. 54, No. 4
0066-4804/10/$12.00 doi:10.1128/AAC.01158-09

Neutrophil Gelatinase-Associated Lipocalin Expresses Antimicrobial Activity by Interfering with L-Norepinephrine-Mediated Bacterial Iron Acquisition[▽]

Marcus Miethke and Arne Skerra*

Munich Center for Integrated Protein Science, CIPS-M, and Lehrstuhl für Biologische Chemie, Technische Universität München, 85350 Freising-Weihenstephan, Germany

Received 15 August 2009/Returned for modification 23 October 2009/Accepted 6 January 2010

L-norepinephrine (NE) is a neuroendocrine catecholamine that supports bacterial growth by mobilizing iron from a primary source such as holotransferrin to increase its bioavailability for cellular uptake. Iron complexes of NE resemble those of bacterial siderophores that are scavenged by human neutrophil gelatinase-associated lipocalin (NGAL) as part of the innate immune defense. Here, we show that NGAL binds iron-complexed NE, indicating physiological relevance for both bacterial and human iron metabolism. The fluorescence titration of purified recombinant NGAL with the $Fe^{III} \cdot (NE)_3$ iron complex revealed high affinity for this ligand, with a K_D of 50.6 nM. In contrast, the binding protein FeuA of *Bacillus subtilis*, which is involved in the bacterial uptake of triscatecholate iron complexes, has a K_D for $Fe^{III} \cdot (NE)_3$ of 1.6 μM, indicating that NGAL is an efficient competitor. Furthermore, NGAL was shown to inhibit the NE-mediated growth of both *E. coli* and *B. subtilis* strains that either are capable or incapable of producing their native siderophores enterobactin and bacillibactin, respectively. These experiments suggest that iron-complexed NE directly serves as an iron source for bacterial uptake systems, and that NGAL can function as an antagonist of this iron acquisition process. Interestingly, a functional FeuABC uptake system was shown to be necessary for NE-mediated growth stimulation as well as its NGAL-dependent inhibition. This study demonstrates for the first time that human NGAL not only neutralizes pathogen-derived virulence factors but also can effectively scavenge an iron-chelate complex abundant in the host.

For the purpose of high-affinity iron acquisition, microbes use a broad array of iron chelators, known as siderophores, that are secreted by their own species, by other microbes, or by the host organism (11, 40, 50). Mammalian pathogens in particular have to cope with strong iron-deprived conditions. There, iron is tightly bound to host proteins, such as serum transferrin, ferritin, or lactoferrin, which leads to an availability of the free metal ion in plasma at concentrations as low as 10^{-24} M (47). Thus, for successful iron acquisition, mammalian pathogens require siderophores with extraordinary affinities.

Among the three general siderophore classes (40), those of the catecholate type have the highest known Fe^{3+} affinities. Two outstanding examples are the triscatecholate siderophores enterobactin (Ent) and bacillibactin (BB) of enteric bacteria such as *Escherichia coli* and *Bacillus* spp., respectively (Fig. 1). These siderophores have extremely high complex formation constants, with log K_f (complex formation constant) = 49 for Ent (35) and log K_f = 47.6 for BB (13). The acute-phase protein NGAL (also known as lipocalin 2 or siderocalin) sequesters both iron-charged Ent and BB with dissociation constants in the range of 0.4 to 0.5 nM (3, 19, 25), which in the case of Ent was shown to be pivotal in the innate immune response to bacterial infection (20).

During coevolution, pathogens evaded NGAL-mediated defense either by the C5 glucosylation of Ent, leading to salmochelins (17, 26), or by developing novel siderophores such as petrobactin (3). However, crystallographic studies revealed that NGAL also is able to bind carboxymycobactins produced by *Mycobacterium* spp. as well as parabactin from *Paracoccus denitrificans* (28), a structural analog of vibriobactin from *Vibrio cholerae* (Fig. 1). Thus, the NGAL pocket shows a certain plasticity for accommodating a heterogeneous set of catecholic and phenolic iron chelators, which raises the question of whether further interactions with ligands of physiological relevance exist.

Interestingly, small catecholic compounds have Fe^{3+} complex formation constants that enable them to abstract iron from transferrin, which has a logarithmic association constant of around 22 (36), and from other iron-binding proteins. The complex formation constant of $Fe^{3+} \cdot (catechol^{2-})_3$, for example, is impressively high, with log K_f = 45.9 (31). Thus, even though the bacterial triscatecholate siderophores clearly show greatly superior iron affinities compared to those of iron-binding host proteins, pathogens may benefit not only from iron that is acquired by their own siderophores but also from related catecholic compounds with chelating activity derived from the host.

Indeed, previous studies have shown that commensal or pathogenic bacteria such as *Escherichia coli* (9, 22, 23), *Salmonella enterica* (6, 60), *Vibrio parahaemolyticus* (42), *Klebsiella pneumoniae* (45), *Pseudomonas aeruginosa* (45), *Enterobacter*

* Corresponding author. Mailing address: Munich Center for Integrated Protein Science, CIPS-M, Lehrstuhl für Biologische Chemie, Technische Universität München, 85350 Freising-Weihenstephan, Germany. Phone: 49 8161 714351. Fax: 49 8161 714352. E-mail: skerra@wzw.tum.de.

▽ Published ahead of print on 19 January 2010.

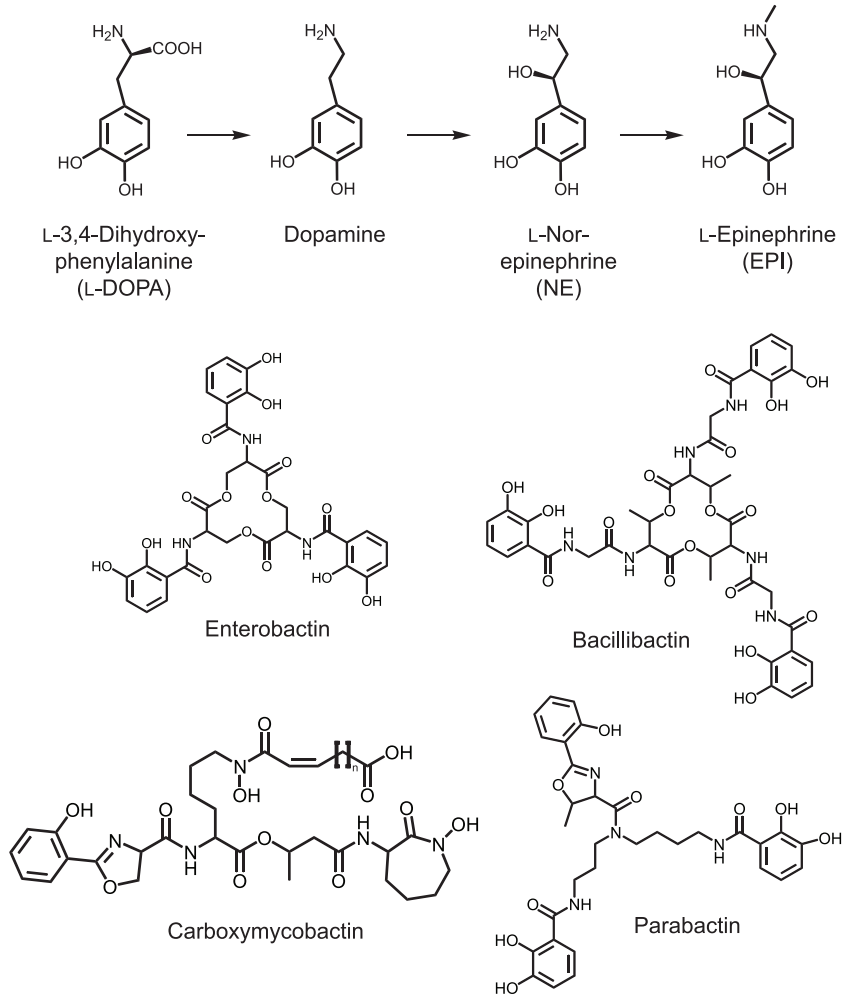

FIG. 1. Chemical structures of neuroendocrine catecholamines shown in the order of their biosynthetic conversion (top), as well as siderophores with known affinity to NGAL (bottom). Enterobactin is produced by enteric bacteria, bacillibactin is produced by *Bacillus* spp., and parabactin is produced by *Paracoccus denitrificans*. Carboxymycobactins are produced by mycobacteria with species-dependent lengths of the carboxyalkyl side chain. In *Mycobacterium tuberculosis*, $n = 1$ to 5; in *Mycobacterium avium*, $n = 2$ to 8; in *Mycobacterium smegmatis*, $n = 2$ to 9.

sp. (45), *Shigella sonnei* (45), *Staphylococcus aureus* (45), *Listeria* spp. (10), and *Bordetella bronchiseptica* (4) utilize neuroendocrine catecholamines such as L-norepinephrine (NE) and L-epinephrine (EPI), as well as their progenitors L-3,4-dihydroxyphenylalanine (L-DOPA) and dopamine (Fig. 1) to acquire iron that is bound to serum transferrin or, in some cases, lactoferrin. Studies with *E. coli* and *S. enterica* suggested that the Ent system is involved in catecholamine-mediated iron acquisition (6, 9, 22).

However, components of the Ent utilization pathway were shown to be downregulated in the presence of NE, possibly due to Fur activation as a result of NE-mediated iron delivery (6, 16). In this context, mutational analyses in *S. enterica* and *E. coli* revealed that the utilization of NE as an iron source depends on the presence of the Cir outer membrane receptor and on the TonB energy system for substrate translocation (22, 60). NE was further shown to complement intragastical Ent- and salmochelin-mediated iron acquisition of *S. enterica* in a mouse model system, leading to the systemic spread of strains with a functional Cir uptake system (60).

In the present study, we demonstrate that iron-complexed L-norepinephrine [$Fe^{III} \cdot (NE)_3$] is tightly bound by NGAL. *E. coli* and *Bacillus subtilis* strains that are deficient in the production of endogenous siderophores are shown to accept NE as an iron source for growth support, with the FeuABC uptake system of *B. subtilis* participating in NE utilization. Growth no longer is supported by NE in cultures supplemented with NGAL, thus suggesting its role as a physiological $Fe^{III} \cdot (NE)_3$ scavenger.

MATERIALS AND METHODS

Recombinant protein production and purification. All proteins were produced in *E. coli* strain BL21 (53). Human NGAL was expressed with N-terminal OmpA signal peptide and C-terminal *Strep*-tag II from the vector phNGAL14 as described previously (8). Alternatively, *Strep*-tag II was exchanged for a C-terminal His_6 tag, yielding the vector pNGAL99. Human tear lipocalin (Tlc) was expressed similarly with N-terminal OmpA signal peptide and the C-terminal *Strep*-tag II from the vector pTlc3 (8). *B. subtilis* FeuA was expressed in the bacterial cytoplasm as C-terminal His_6 tag fusion protein from vector pOK01 (39).

Recombinant NGAL and Tlc were purified from the periplasmic cell extract as

previously described (8). For the production of FeuA, cells were grown in shake flask cultures at 30°C under agitation in LB medium containing 50 μg/ml kanamycin (Kan). At an optical density at 550 nm (OD_{550}) of 0.7, 0.1 mM isopropyl-β-D-thiogalactopyranoside (IPTG) was added to induce gene expression, which was continued for 4 h. Cells were harvested and resuspended in 100 mM NaCl, 50 mM NaP_i, pH 7.5. Cells then were disrupted by means of a French press, and debris were removed by centrifugation. The clear supernatant was applied onto an IDA-Sepharose column (GE Healthcare, Munich, Germany) charged with $ZnSO_4$, and the His_6-tagged protein was eluted with a linear imidazole concentration gradient from 0 to 250 mM in 100 mM NaCl, 50 mM NaP_i, pH 7.5. Elution fractions were pooled, concentrated by ultrafiltration, and applied to gel filtration in the presence of 100 mM NaCl, 10 mM Tris-HCl, pH 8.0, on a HiLoad 16/60 Superdex 75 column using an Äkta purifier system (GE Healthcare). To remove a contamination of slightly smaller size, the fractions containing the recombinant FeuA (pI = 7.2) were dialyzed against 20 mM Tris-HCl, pH 8.5, and loaded onto a 1-ml Resource Q column (GE Healthcare) on an Äkta purifier system. Elution was performed with a linear NaCl concentration gradient from 0 to 500 mM in 20 mM Tris-HCl, pH 8.5, over 40 column volumes at a flow rate of 1 ml/min. Elution fractions were analyzed by SDS-PAGE, and pure fractions were pooled and dialyzed against 100 mM NaCl, 10 mM Tris-HCl, pH 8.0. The protein concentration was determined using a molar extinction coefficient as previously reported (39).

Fluorescence titration. Fluorescence titration studies were performed essentially as previously described (8). The protein solution in 100 mM NaCl, 10 mM Tris-HCl, pH 8.0, was adjusted to the desired concentration, and 2 ml of this solution was applied to a 1- by 1-cm^2 quartz cuvette. The cuvette was placed into a Fluoro-Max 3 spectrofluorimeter (Horiba Jobin Yvon, Longjumeau, France) and thermostatted at 20°C. Ligand stock solutions concentrated 2,000-fold [200-fold in the case of FeuA titration with NE or $Fe^{III} \cdot (NE)_3$] with respect to the molar protein concentration were freshly prepared in H_2O. Siderophore ligands enterobactin (Ent) and bacillibactin (BB) were obtained in synthetic form or were isolated from bacterial cultures, respectively, as previously described (18, 39). Catecholamines L-norepinephrine (NE), L-epinephrine (EPI), L-DOPA, and dopamine were purchased (Alfa Aesar, Karlsruhe, Germany). For charging with iron, ligand solutions were mixed with a fresh $FeCl_3$ (Sigma-Aldrich, Munich, Germany) solution in H_2O at the appropriate molar stoichiometry, followed by incubation for 5 min at 20°C. Defined amounts of the iron-ligand solution then were added stepwise to the protein solution. After each titration step, the solution was mixed for 3 min by magnet stirring in the cuvette and then rested for another 2 min before fluorescence was measured. The protein Tyr/Trp fluorescence was excited at 280 nm (slit width, 5 nm) and detected at 340 nm (slit width, 10 nm). Each measurement was averaged for 10 s. In the case of iron-charged enterobactin and bacillibactin, ligand absorption was corrected after analogous titration with a 5 μM *N*-acetyl-tryptophanamide solution as described previously (59). For the analysis of the fluorescence titration series, data were set to a 100% starting fluorescence intensity and fitted according to the law of mass action for bimolecular complex formation (57) by nonlinear regression analysis (KaleidaGraph software) using the equation

$$F = ([P]_t - [L]_t - K_D)\frac{f_P}{2} + ([L]_t - [P]_t - K_D)\frac{f_L}{2} + ([P]_t + [L]_t + K_D)\frac{f_{PL}}{2} + (f_P + f_L - f_{PL})\sqrt{\frac{([P]_t + [L]_t + K_D)^2}{4} - [P]_t[L]_t} \quad (1)$$

where $[P]_t$ and $[L]_t$ are total protein and ligand concentrations at each titration step, respectively; f_P, f_L, and f_{PL} are the relative molar fluorescence coefficients of the free protein, the free ligand, and the protein-ligand complex, respectively; and K_D is the dissociation constant. K_D and f_{PL} were set as free parameters, while f_P was adjusted to the starting fluorescence without ligand (e.g., 100%/μM). In the case of iron-catecholamine complexes, f_L was set as an additional free parameter to account for intrinsic ligand fluorescence. All titrations also were carried out with either bovine serum albumin (BSA; Sigma-Aldrich) as a control protein or $FeCl_3$ as a control ligand.

Cell growth assays. *B. subtilis* strains ATCC 21332 (37), Δ*dhbC* (BMM100), and Δ*dhbC* Δ*feuABC* (BMM111) (39) were grown in Belitsky minimal medium (54) with 0.5% (wt/vol) glucose, 4.5 mM Na-glutamate, with the omission of citrate and iron salts. *E. coli* strains MC4100 (63) and Δ*entC* (H5687) (63) were grown in SAPI minimal medium (9) with 0.1% (wt/vol) glucose and 0.001% (wt/vol) thiamine, again with the omission of iron salts. Colonies from each strain freshly grown on LB plates (49) were used for the inoculation of minimal medium, followed by incubation in polypropylene culture tubes at 37°C and 200 rpm for about 12 h. The cell densities of the iron-limited overnight cultures were measured, and cultures were diluted with fresh minimal medium to 10^3 CFU/ml. Diluted cultures then were transferred into 96-well round-bottom polystyrene plates (Nunc, Wiesbaden, Germany) to 100 μl/well. Additional components, i.e., NGAL, Tlc, apotransferrin (apoTf; ICN Biomedicals, Eschwege, Germany), holotransferrin (holoTf; Calbiochem, Darmstadt, Germany), NE, EPI, and $FeCl_3$, were supplemented in three independent wells for each combination or concentration tested. Empty wells were filled with 100 μl sterile medium for the control of contamination and to ensure the homogeneity of a humid atmosphere. Plates were incubated with a lid at 37°C and 500 rpm for 20 h on a microtiter plate shaker (Eppendorf, Hamburg, Germany). For viable cell counting, 20-μl samples were taken from each well, including three controls. Eight successive 10-fold dilutions were made from each sample using sterile medium, followed by plating onto LB agar. Colony counts for each triplicate were averaged and plotted with the corresponding standard deviations. For the determination of half-maximal inhibitory concentrations (IC_{50}), colony averages from inhibition cultures were related to those obtained without the addition of inhibitor, and curves were plotted and analyzed according to the model of logarithmic dose-response (Origin software) using the sigmoidal equation

$$\frac{cfu_i}{cfu_c} = \frac{(A_{max} - A_{min})}{1 + \left(\frac{[I]_{tot}}{IC_{50}}\right)^p} + A_{min} \quad (2)$$

where cfu_i and cfu_c are the averaged cell counts of inhibition and control cultures, respectively, A_{max} and A_{min} are the top and the bottom parameters of the curve, respectively, $[I]_{tot}$ is the total inhibitor concentration, and p is the logarithmic slope.

Protein crystallization and ligand soaking. A 24.8-mg/ml solution of purified recombinant NGAL carrying the C-terminal *Strep*-tag II in 100 mM NaCl, 10 mM Tris-HCl, pH 8.0, was subjected to hanging drop vapor diffusion crystallization in combination with microseeding at 20°C (38). Crystals were obtained in the presence of 0.1 M Bis/Tris-HCl, pH 5.5, 34.5% (wt/vol) polyethylene glycol (PEG) 3350. Ligand soaking was performed for about 24 h under a nitrogen atmosphere by transferring crystals into fresh precipitant solution containing 0.44 mM $Fe^{III} \cdot (NE)_3$ and, to prevent ligand precipitation, having a higher pH (0.1 M HEPES-NaOH, pH 7.5, 34.5% [wt/vol] PEG 3350).

RESULTS

Binding of iron-complexed NE to NGAL and FeuA. Since NGAL is known as a high-affinity scavenger of bacterial catecholate and phenolate siderophores, we investigated whether this protein also is capable of sequestering iron-chelating host molecules with chemically related structures. In this regard, neuroendocrine catecholamines, which often are utilized by microbes as iron sources, appeared to be of particular interest. Thus, corresponding binding studies were performed by the fluorescence titration of recombinant NGAL (Fig. 2). Titration with iron-complexed NE led to a pronounced fluorescence quenching effect (Fig. 3). After correction for the intrinsic fluorescence of catecholamine complexes (44), a K_D value of 50.6 ± 9.3 nM (Table 1) was determined for the interaction between the preformed $Fe^{III} \cdot (NE)_3$ complex (31) and NGAL.

In contrast to NE, titration with iron-complexed EPI (Fig. 3B) and also with L-DOPA (not shown) did not result in detectable fluorescence quenching, indicating that the iron complexes of these catecholamines do not bind to NGAL with significant affinity. As expected, titration with the known ligands $Fe^{III} \cdot$ Ent and $Fe^{III} \cdot$ BB led to strong fluorescence quenching (Fig. 3C, D), and the resulting K_D values of 0.40 ± 0.15 and 0.52 ± 0.16 nM, respectively, are in agreement with previous reports (3, 25). Titration with dopamine was not possible, since its complexation with Fe^{3+} led to a precipitate, possibly due to metal-catalyzed melanine formation (34).

Although bacteria have been described to utilize iron mobilized by NE and other catecholamines, it still is unclear to what

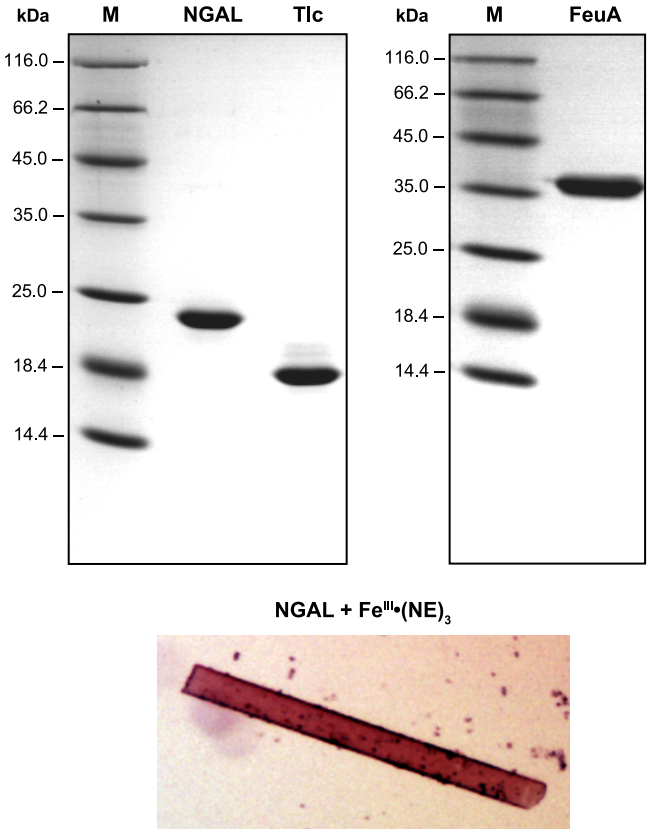

FIG. 2. SDS-PAGE of purified proteins used in this study. The recombinant proteins NGAL and Tlc, both fused at the C terminus with the *Strep*-tag II, as well as FeuA fused at the C terminus with the His_6 tag, all were produced in *E. coli*. M, protein size marker. At the bottom, the soaking of an apoNGAL crystal with $Fe^{III} \cdot (NE)_3$ resulted in a deep red color, which indicates binding to the ligand pocket of the lipocalin.

extent iron-complexed catecholamines directly serve as substrates for bacterial uptake systems. Thus, the substrate binding protein FeuA of *B. subtilis*, an extracytoplasmic lipoprotein that scavenges iron-charged triscatecholate siderophores prior to their uptake via the FeuBC/YusV membrane permease/ATP-binding cassette complex (39, 46), was tested for its ability to recognize iron-complexed NE. Titration of the recombinant FeuA (Fig. 2) with $Fe^{III} \cdot (NE)_3$ resulted in fluorescence quenching (Fig. 3E) with a K_D of 1.6 ± 0.2 μM, whereas the titration of FeuA with its native ligand $Fe^{III} \cdot$ BB yielded a lower K_D of 26.5 ± 1.4 nM (Fig. 3F), which is in agreement with earlier measurements (39). Notably, the 30-fold-lower affinity of FeuA for $Fe^{III} \cdot (NE)_3$ compared to that of NGAL indicates that the latter can act as a potent competitor in binding of this iron complex. The titration of NGAL and FeuA with catecholamine ligands in the absence of Fe^{3+} did not lead to detectable fluorescence quenching, while titration with $FeCl_3$ in the higher-micromolar range resulted in unspecific quenching both of the test proteins and of BSA, which served as a negative control.

In earlier experimental studies, the soaking of NGAL protein crystals with iron-complexed siderophores was accompanied by a color change to red-brown, qualitatively indicating accommodation in the ligand pocket of this lipocalin (2, 3, 19). Consequently, we soaked freshly grown crystals of the recombinant NGAL with $Fe^{III} \cdot (NE)_3$ at pH 7.5 and, indeed, the crystals turned from colorless to deep red, while the crystal morphology remained unaffected (Fig. 2). This observation further supports that iron-complexed NE tightly binds to NGAL in a most likely native conformation, which also should allow the structural elucidation of the complex via X-ray crystallography in the future.

Growth of *E. coli* and *B. subtilis* strains in the presence of NE and NGAL. *E. coli* MC4100 and *B. subtilis* ATCC 21332 were used as Gram-negative and Gram-positive model strains, respectively, which synthesize the natural triscatecholate siderophores Ent and BB. Since these siderophores are considered the major targets of sequestration by NGAL (3, 25), cross-binding effects were avoided by using mutant strains deficient in siderophore biosynthesis. The *E. coli* Δ*entC* and *B. subtilis* Δ*dhbC* mutants lack isochorismate synthase activity (39, 63), thus abolishing the biosynthesis of both the triscatecholate siderophores and their common precursor 2,3-dihydroxybenzoate (DHB), an alternative siderophore that can form an $Fe^{III} \cdot (DHB)_3$ complex recognized by NGAL (25).

In a first growth experiment, iron-limited cultures with 10^3 CFU/ml starting inocula were supplemented with 50 μM NE, holotransferrin (holoTf), apotransferrin (apoTf), NGAL, and $FeCl_3$ in different combinations. An NE concentration of 50 μM previously was identified to be optimal for the growth of *E. coli* under similar *in vitro* conditions (9) and furthermore corresponds to the physiological situation, for example, during traumatic injury *in vivo* (24, 55, 56). The concentration of 50 μM for Tf was chosen according to its abundance *in vivo* (48). After 20 h of culture growth, viable plate counts were determined and CFU were plotted (Fig. 4).

Neither wild-type (WT) nor mutant strains responded to the addition of NE alone. WT strains were growth stimulated by the addition of holoTf and, in contrast, showed reduced growth when NGAL was added to the cultures. The effects of holoTf and NGAL on WT growth indicated the involvement of their endogenous siderophores in iron acquisition, because the siderophore-deficient mutant strains did not respond to holoTf or NGAL alone. Interestingly, the mutants showed increased growth upon the combined addition of NE and holoTf, indicating that NE is sufficient to mobilize iron from holoTf for bacterial growth without the need of an endogenous siderophore or precursor. However, the triple combination of NE, holoTf, and NGAL led to a significant growth inhibition of WT as well as mutant strains, in particular when NGAL was added at a higher concentration (Fig. 4C), thus demonstrating its antimicrobial activity.

Control cultures supplemented with apoTf alone or in combination with NE had no significant effect on growth (Fig. 4A, B). The marginal growth stimulation of apoTf in combination with NE in the mutant cultures may have been due to residual iron contamination of the *apo* protein. Supplementation with $FeCl_3$ led to growth enhancement in all cultures. However, no inhibition was observed in this case upon the addition of NGAL, confirming that the antimicrobial effect of NGAL is confined to conditions of iron limitation, under which siderophore-mediated iron acquisition is crucial.

The NGAL concentrations needed for half-maximal growth

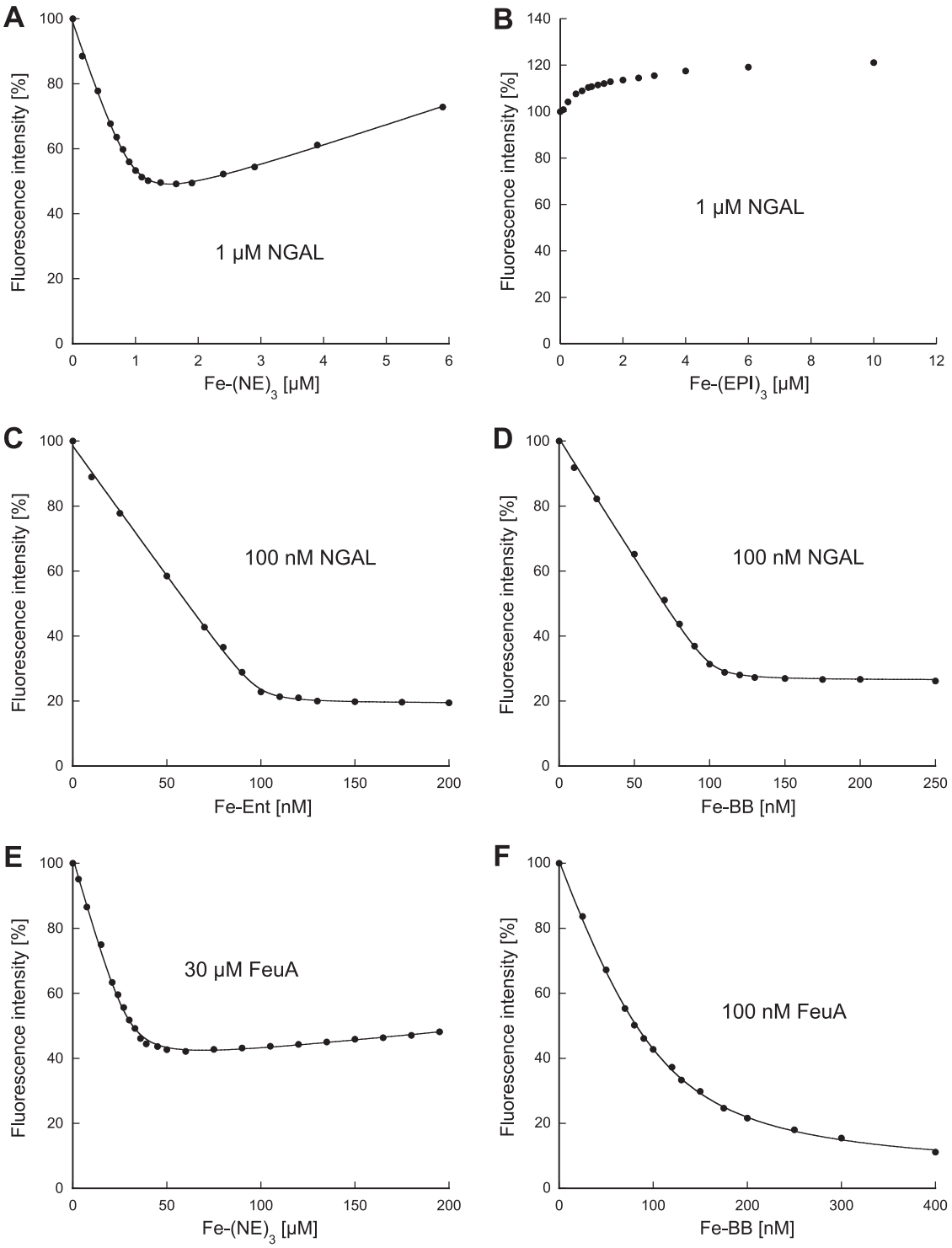

FIG. 3. Fluorescence titration of recombinant NGAL and FeuA with bacterial siderophores or neuroendocrine catecholamines. (A) One μM NGAL was titrated with the preformed Fe^{3+} complex of L-norepinephrine [$Fe^{III} \cdot (NE)_3$]. (B) One μM NGAL was titrated with the preformed Fe^{3+} complex of L-epinephrine [$Fe^{III} \cdot (EPI)_3$]. (C) NGAL (100 nM) was titrated with Fe^{III} · enterobactin (Fe^{III} · Ent). (D) NGAL (100 nM) was titrated with Fe^{III} · bacillibactin (Fe^{III} · BB). (E) FeuA (30 μM) was titrated with $Fe^{III} \cdot (NE)_3$. (F) FeuA (100 nM) was titrated with Fe^{III} · BB. In all cases, Tyr/Trp fluorescence was excited at 280 nm and detected at 340 nm. Data were fit according to the law of mass action to determine the dissociation constants for protein-ligand complex formation (Table 1).

TABLE 1. Dissociation constants of protein-ligand complexes determined by fluorescence titration

Protein	Ligand	K_D [nM]
NGAL	$Fe^{III} \cdot (norepinephrine)_3$	50.6 ± 9.3
	$Fe^{III} \cdot (epinephrine)_3$	–[a]
	$Fe^{III} \cdot$ enterobactin	0.4 ± 0.15
	$Fe^{III} \cdot$ bacillibactin	0.52 ± 0.16
Tlc	$Fe^{III} \cdot (norepinephrine)_3$	–
	$Fe^{III} \cdot$ enterobactin	243.3 ± 50.7
FeuA	$Fe^{III} \cdot (norepinephrine)_3$	1,600 ± 200
	$Fe^{III} \cdot$ bacillibactin	26.5 ± 1.4

[a] –, no binding observed.

inhibition under those conditions, i.e., in the presence of 50 μM NE and 50 μM holoTf, were assessed in a separate experiment, resulting in IC_{50} values of 12.4 ± 1.4 and 73.3 ± 8.7 μM for *B. subtilis* WT and Δ*dhbC* strains and of 160.0 ± 14.2 and 211 ± 10.3 μM for *E. coli* WT and Δ*entC* strains, respectively (Fig. 5). These findings support a direct competitive effect between the bacterial uptake of iron-complexed NE and sequestration by NGAL.

Bacterial growth in the presence of EPI and Tlc. Similarly to NGAL, Tlc is a member of the lipocalin family that exhibits the overall β-barrel fold with a central ligand pocket (7) and acts as a scavenger of microbial siderophores (21). In contrast to the plasma protein NGAL, however, Tlc mainly occurs in secretory fluids and its ligand spectrum is broader, with generally lower affinities. To test the effect of Tlc on NE-dependent growth, recombinant Tlc was produced and purified under similar conditions (Fig. 2) and was added in various concentrations to cultures supplemented with NE and holoTf (Fig. 4C). In contrast to the addition of NGAL, which significantly reduced NE-dependent growth enhancement in Δ*dhbC* or Δ*entC* strains, the addition of Tlc had no detectable growth effect.

The influence of NGAL and Tlc also was tested in cultures supplemented with EPI and holoTf (Fig. 4D). The growth enhancement observed in the presence of EPI and holoTf was comparable to NE-dependent growth stimulation. However, in this case, the addition of neither NGAL nor Tlc led to an inhibitory effect, indicating that EPI is not accessible for sequestration by both lipocalins. Tlc was further subjected to fluorescence titration with Fe^{3+} complexes of Ent, NE, and EPI. While titration with $Fe^{III} \cdot$ Ent resulted in detectable

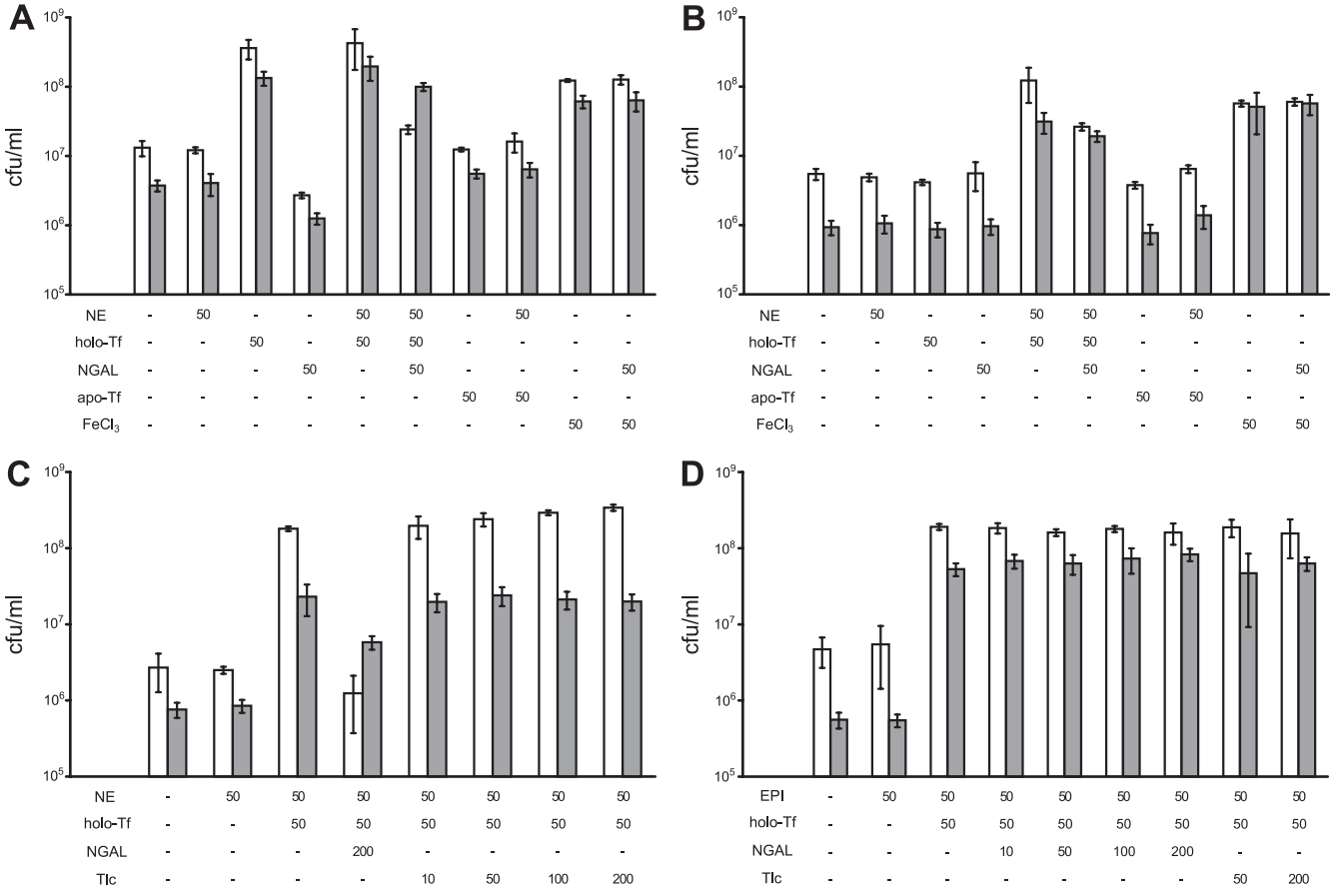

FIG. 4. Cell growth assays with *B. subtilis* and *E. coli* wild-type (WT) and siderophore biosynthesis mutant strains. (A) Colony counts of *B. subtilis* WT (white bars) and *E. coli* WT (gray bars) cultures. (B to D) Colony counts of *B. subtilis* Δ*dhbC* (white bars) and *E. coli* Δ*entC* (gray bars) cultures. Strains were grown in iron-limited minimal medium with initial inocula of 10^3 CFU/ml. Test supplements were made in different combinations and ligand concentrations (in μM) as indicated below the columns. After cultivation for 20 h, viable cells were counted. Bars represent average values of three independent biological experiments. Error bars indicate the corresponding standard deviations.

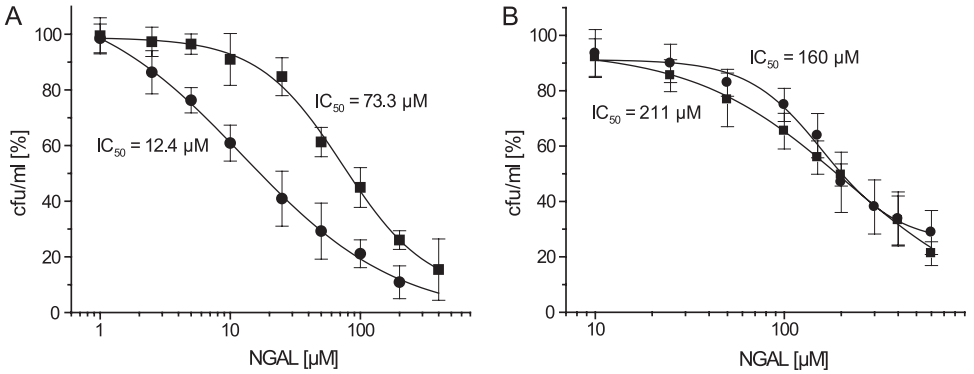

FIG. 5. Determination of half-maximal inhibitory concentrations (IC_{50}) of NGAL with respect to bacterial growth in iron-limited cultures in the presence of 50 μM NE and 50 μM holoTf. (A) Dose-response curves of *B. subtilis* WT (filled circles) and Δ*dhbC* (filled squares) cultures. (B) Dose-response curves of *E. coli* WT (filled circles) and Δ*entC* (filled squares) cultures. Viable cell counts for each NGAL concentration were related to cell counts of control cultures in the absence of NGAL (corresponding to 100%). All data points represent average values of three independent biological replicates, and error bars indicate the corresponding standard deviations.

fluorescence quenching, yielding a K_D of 243.3 ± 50.7 nM, no quenching was observed with the iron-complexed catecholamines, indicating a lack of significant affinity.

The FeuABC uptake system is involved in NE-mediated iron acquisition. The fluorescence titration studies had shown that the bacterial triscatecholate binding protein FeuA possesses affinity for iron-complexed NE (Fig. 3E). Since the FeuABC transport system serves for the uptake of triscatecholic iron chelators in *B. subtilis* (39, 46), we tested whether an *feuABC* deletion influences NE-dependent growth enhancement and its inhibition in the presence of NGAL. The transporter deletion was introduced into the biosynthesis mutant Δ*dhbC*, yielding a Δ*dhbC* Δ*feuABC* double mutant, and both strains were grown with the addition of NE, EPI, holoTf, NGAL, and Tlc in different combinations (Fig. 6).

While Δ*dhbC* showed NE- and EPI-dependent growth enhancement in the presence of holoTf, the catecholamine-dependent stimulation of growth clearly was impaired in the Δ*dhbC* Δ*feuABC* background. In contrast, NGAL-mediated inhibition in a concentration-dependent manner was observed for NE-supplemented, but not for EPI-supplemented, Δ*dhbC* cultures, whereas this effect was abolished in the Δ*dhbC* Δ*feuABC* double mutant. This strongly indicated that the FeuABC uptake system is involved in the utilization of iron-complexed catecholamines to acquire iron for cellular growth. In accordance with the fluorescence titration experiment, the missing NGAL-dependent cellular growth inhibition with holoTf/NE as the iron source in the absence of FeuABC indicates that the antimicrobial effect is due essentially to a direct competition for iron-complexed NE between NGAL and the FeuA(BC) uptake system of *B. subtilis*.

DISCUSSION

The bacterial utilization of neuroendocrine catecholamines as an iron source is an important aspect of microbe-host interactions. These compounds are abundant in all mammalian hosts such that pathogens could further benefit from increased

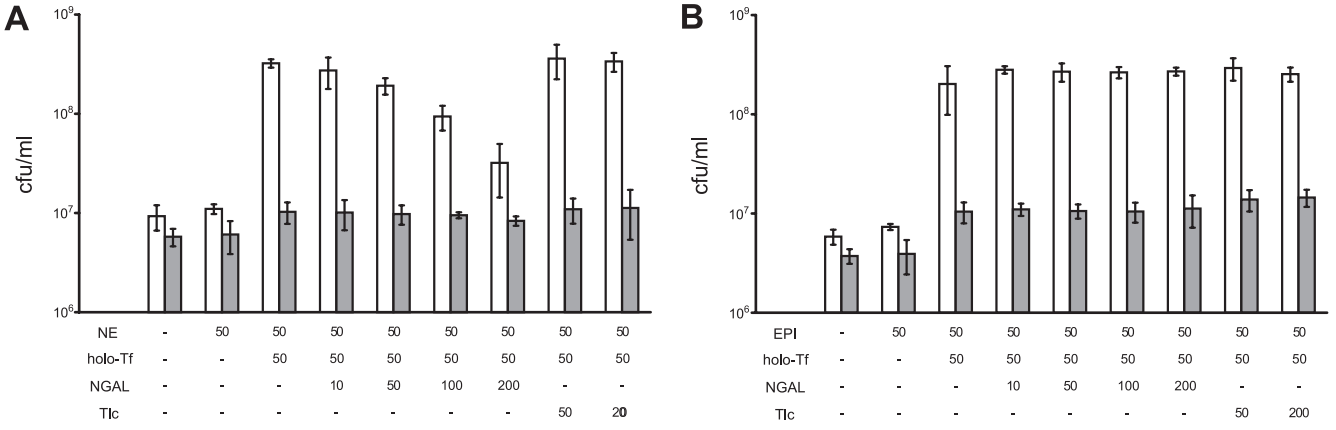

FIG. 6. Cell growth assays with mutant strains of *B. subtilis*, Δ*dhbC* and Δ*dhbC* Δ*feuABC*, defective in siderophore biosynthesis and siderophore biosynthesis as well as triscatecholate uptake, respectively. (A) Colony counts of *B. subtilis* Δ*dhbC* (white bars) and Δ*dhbC* Δ*feuABC* (gray bars) cultures in the presence of NE. (B) Colony counts of *B. subtilis* Δ*dhbC* (white bars) and Δ*dhbC* Δ*feuABC* (gray bars) cultures in the presence of EPI. Strains were grown in iron-limited minimal media with initial inocula of 10^3 CFU/ml. Supplements were made to the cultures in micromolar concentrations as indicated below the columns. After cultivation for 20 h, viable cells were counted. Bars represent mean values of three independent biological replicates, and error bars indicate the corresponding standard deviations.

levels during stress or disease states. For example, severe tissue damage in trauma or burn patients causes massive systemic release of NE that can spill over into the intestine, where commensal bacteria that otherwise are limited in iron availability frequently cause intraabdominal sepsis (23, 24).

In the present study, NE-mediated bacterial growth stimulation was observed in siderophore-deficient strains of *E. coli* and *B. subtilis*, demonstrating that NE can be utilized as a host-derived iron source that mobilizes this essential element from primary sources such as holoTf. In fact, NE previously was shown to effectively liberate iron from holoTf under dialysis conditions (22). In *B. bronchiseptica*, NE alone is sufficient to stimulate cellular growth in serum-supplemented medium and probably is taken up in a TonB-dependent manner, whereas the BfeA outer membrane receptor (OMR), which is NE inducible, is not required for growth stimulation (4, 5).

In *E. coli*, the utilization of NE as a direct iron source seems to be strain specific, since defective Ent biosynthesis did not result in NE-dependent growth stimulation in the mutant strains AN193 *entA*$^-$ (9) and NCTC12900 (O157:H7) *entA*$^-$ (22). However, radiolabeling experiments with [^{3}H]NE and [^{55}Fe]Tf resulted in the intracellular detection of both tritiated NE and the ^{55}Fe isotope in strain E2348/69 (O127:H6), thus proving the potential for cellular uptake of iron-complexed NE (23). Notably, when an *S. enterica iroN fepA* double mutant was compared to an *iroN fepA cir* triple mutant, the latter was not growth supported by NE *in vivo* (60), indicating that the ability of direct $Fe^{III} \cdot (NE)_3$ utilization varies with the individual uptake systems present in *E. coli* and its relatives. Nevertheless, these experiments showed that the Cir outer membrane receptor is crucial for NE utilization, which is in agreement with its ability to utilize the structurally related 2,3-dihydroxybenzoylserine as an iron source (26).

The virulence-related role of compounds such as NE or EPI, important hormones and neurotransmitters in the peripheral and central nervous system, illustrates the necessity for the host to control the overall availability of these compounds, in particular in the context of inflammation-associated physiological responses. In this respect, the present study demonstrates that the acute-phase protein NGAL is able to sequester iron-complexed NE and counteract NE-stimulated growth, which could provide the protection of the host against catecholamine-dependent pathogen spreading, at least in compartments where holoTf and NE are abundant (12, 36).

The affinity of NGAL for $Fe^{III} \cdot (NE)_3$ was found to be significantly higher than that of bacterial FeuA, and indeed, competition with bacterial uptake, in particular via FeuABC, was demonstrated here by means of systematic growth analyses. On the other hand, Tlc, which previously was identified as another siderophore-binding protein in mammals, is unlikely to be involved in $Fe^{III} \cdot (NE)_3$ sequestration. This underlines the distinct physiological properties of lipocalin family members even in the case of ligands with related structure and function (8).

The NGAL concentrations needed to achieve half-maximal bacterial growth inhibition were found to be in the micromolar range. In this context, it should be noted that affinities of OMRs such as FepA, which possesses a K_D of <0.2 nM for $Fe^{III} \cdot$ Ent, often are impressively high (43). Hence, the elevated NGAL concentrations needed for growth inhibition in *E. coli* cultures are consistent with an effective competition of the OMRs for their iron-triscatecholate substrates. Since high NGAL concentrations not only were necessary to compete with FepA-mediated $Fe^{III} \cdot$ Ent uptake in the WT strain but also to effectively inhibit the growth of Δ*entC* in response to NE, an affinity similarly tight as that known between FepA and $Fe^{III} \cdot$ Ent has to be anticipated for Cir and the iron-NE complex. In contrast, NGAL was found to compete more effectively with iron uptake in *B. subtilis*, which is in agreement with the general observation that substrate-binding proteins at the extracellular leaflet of the cytoplasmic membrane have lower affinities than OMRs recognizing the same substrate(s) (40). As an example, *E. coli* FepA has about 100-fold higher affinity for $Fe^{III} \cdot$ Ent than the periplasmic binding protein FepB and its homolog FeuA (39, 52, 62).

Furthermore, enhanced NGAL-dependent growth inhibition in the WT cultures may result not only from the preferred binding of endogenously produced siderophores over exogenously supplied NE to the lipocalin but also from the preferred utilization of the native siderophores by bacterial triscatecholate binding proteins, such as *B. subtilis* FeuA or *E. coli* FepB, as shown by protein-ligand binding experiments in this and previous studies (39, 52).

Interestingly, although *B. subtilis* is a close relative of mammalian pathogens such as *B. anthracis* and *B. cereus*, it is a nonpathogenic bacterium that widely occurs in soil habitats. However, the present study shows that during iron-limited conditions, its growth is supported by catecholamines, such as NE and EPI. This becomes more reasonable considering that these compounds also are abundant in nonmammalian organisms, in particular soil-dwelling invertebrates (32, 58), and even in plants (33). In this context, catecholamines and their derivatives may represent important iron-mobilizing compounds for microbes living in the soil and other habitats outside mammalian hosts, a possibility that has not been considered so far.

Earlier binding experiments with $Fe^{III} \cdot (2,3\text{-DHB})_3$ and $Fe^{III} \cdot (3,4\text{-DHB})_3$ suggested that 3,4-substituted catecholic ligands cause steric conflicts within the ligand pocket of NGAL (3). However, as we were able to detect the binding of $Fe^{III} \cdot (NE)_3$ to NGAL in solution and also observed the coloring of protein crystals upon soaking, it is possible that the precise arrangement of the substituents protruding from the aromatic ring plays a more important role than previously assumed (27). In fact, the modeling of $Fe^{III} \cdot (NE)_3$ indicates that at least the lower part of this complex, which should reside at the bottom of the ligand pocket considering the crystal structure with bound $Fe^{III} \cdot$ Ent (25), has a rather similar molecular shape and probably can undergo the same interactions with NGAL (Fig. 7). However, the geometry of the ligand complex should be more flexible in the case of $Fe^{III} \cdot (NE)_3$, because the three individual metal-chelating groups are not covalently cross-linked. To elucidate the exact mode of binding to NGAL, crystallographic studies in the presence of $Fe^{III} \cdot (NE)_3$ are under way.

In addition to antimicrobiosis, the sequestration of iron-complexed NE by NGAL is the first example for the interaction of a host-derived ligand with this innate defense protein. The interaction of NGAL with siderophore-like host compound(s) previously was postulated, as this lipocalin extensively participates in iron trafficking throughout the body and is

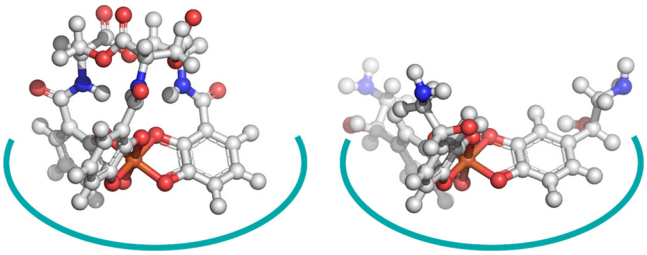

FIG. 7. Structural comparison of the $Fe^{III} \cdot (NE)_3$ complex with $Fe^{III} \cdot$ Ent. The coordinate set of $Fe^{III} \cdot$ Ent was taken from a partially refined crystal structure of its complex with NGAL (PDB entry 1IL6; courtesy of R. Strong) and energy minimized with CS Chem3D Pro 4.0 (left). Its interface with the ligand pocket of NGAL is indicated by the green line. The $Fe^{III} \cdot (NE)_3$ complex was modeled starting from a similar geometry using the same software (right). Obviously, $Fe^{III} \cdot (NE)_3$ would be able to form similar cation-π interactions, as they have been described for $Fe^{III} \cdot$ Ent bound to NGAL (25), even though the accommodation of the catechol side chains of NE might require some steric rearrangement at the opening of the ligand pocket. Illustrations were prepared with PyMOL (carbon and hydrogen, white; oxygen, red; nitrogen, blue; iron, orange; De Lano Scientific).

associated with physiological processes (41, 51). Indeed, NGAL seems to deliver scavenged iron-chelate complexes, such as $Fe^{III} \cdot$ Ent, to the liver, the proximal tubules of the kidney, and the placenta via several endocytic pathways involving cell surface receptors such as megalin (29) and 24p3R (14). Furthermore, it was shown that the uptake of NGAL in complex with $Fe^{III} \cdot$ Ent via 24p3R increases the intracellular iron pool, while the uptake of apoNGAL diminishes intracellular iron levels, which leads to cellular apoptosis (14, 15). NGAL-mediated iron trafficking can sufficiently complement Tf-mediated iron delivery, as observed in the metanephric mesenchyme, and has important physiological consequences, such as antiapoptotic effects for epithelial progenitors (61) and thyroid tumor cells (30).

Hence, it was proposed that mammals possess endogenous iron chelators that, similarly to enterobactin, may reside intracellularly (14) or are secreted and can extracellularly charge NGAL with iron. Indeed, siderophore-like activities were observed in the urine of humans, dogs, and mice, and a catechol-like constitution was anticipated for the responsible molecule(s) (51).

In light of our present findings, it is conceivable that catecholamines such as NE act as iron ligands for NGAL as part of physiological iron trafficking and delivery processes. Intracellular iron release from *holo*-NGAL after uptake into acidic endosomes should be possible with the acid-labile $Fe^{III} \cdot (NE)_3$ complex in the same way as it was recently shown for the bacterial $Fe^{III} \cdot$ Ent ligand (1). Thus, the present study suggests a role of the NGAL/$Fe^{III} \cdot (NE)_3$ complex formation beyond pathogen defense, which deserves further investigation in the context of NGAL-mediated iron homeostasis.

ACKNOWLEDGMENTS

We thank M. A. Marahiel (University of Marburg, Germany) for kindly providing *B. subtilis* strains, K. Hantke (University of Tübingen, Germany) for kindly providing strain *E. coli* H5687, and C. T. Walsh and M. A. Fischbach (Harvard Medical School, Boston, MA) for kindly providing synthetic enterobactin. The support by H. J. Kim during recombinant NGAL expression and characterization and by A. Eichinger and W. Meining (all at Technische Universität München) for help with protein crystallization is gratefully acknowledged.

This work was supported by a DFG research fellowship (MI 1265/1-1) to M.M.

REFERENCES

1. **Abergel, R. J., M. C. Clifton, J. C. Pizarro, J. A. Warner, D. K. Shuh, R. K. Strong, and K. N. Raymond.** 2008. The siderocalin/enterobactin interaction: a link between mammalian immunity and bacterial iron transport. J. Am. Chem. Soc. **130:**11524–11534.
2. **Abergel, R. J., E. G. Moore, R. K. Strong, and K. N. Raymond.** 2006. Microbial evasion of the immune system: structural modifications of enterobactin impair siderocalin recognition. J. Am. Chem. Soc. **128:**10998–10999.
3. **Abergel, R. J., M. K. Wilson, J. E. Arceneaux, T. M. Hoette, R. K. Strong, B. R. Byers, and K. N. Raymond.** 2006. Anthrax pathogen evades the mammalian immune system through stealth siderophore production. Proc. Natl. Acad. Sci. USA **103:**18499–18503.
4. **Anderson, M. T., and S. K. Armstrong.** 2006. The *Bordetella* Bfe system: growth and transcriptional response to siderophores, catechols, and neuroendocrine catecholamines. J. Bacteriol. **188:**5731–5740.
5. **Anderson, M. T., and S. K. Armstrong.** 2008. Norepinephrine mediates acquisition of transferrin-iron in *Bordetella bronchiseptica*. J. Bacteriol. **190:**3940–3947.
6. **Bearson, B. L., S. M. Bearson, J. J. Uthe, S. E. Dowd, J. O. Houghton, I. Lee, M. J. Toscano, and D. C. Lay, Jr.** 2008. Iron regulated genes of *Salmonella enterica* serovar Typhimurium in response to norepinephrine and the requirement of *fepDGC* for norepinephrine-enhanced growth. Microbes Infect. **10:**807–816.
7. **Breustedt, D. A., I. P. Korndörfer, B. Redl, and A. Skerra.** 2005. The 1.8-Å crystal structure of human tear lipocalin reveals an extended branched cavity with capacity for multiple ligands. J. Biol. Chem. **280:**484–493.
8. **Breustedt, D. A., D. L. Schönfeld, and A. Skerra.** 2006. Comparative ligand-binding analysis of ten human lipocalins. Biochim. Biophys. Acta **1764:**161–173.
9. **Burton, C. L., S. R. Chhabra, S. Swift, T. J. Baldwin, H. Withers, S. J. Hill, and P. Williams.** 2002. The growth response of *Escherichia coli* to neurotransmitters and related catecholamine drugs requires a functional enterobactin biosynthesis and uptake system. Infect. Immun. **70:**5913–5923.
10. **Coulanges, V., P. Andre, and D. J. Vidon.** 1998. Effect of siderophores, catecholamines, and catechol compounds on *Listeria* spp. Growth in iron-complexed medium. Biochem. Biophys. Res. Commun. **249:**526–530.
11. **Crosa, J. H., and C. T. Walsh.** 2002. Genetics and assembly line enzymology of siderophore biosynthesis in bacteria. Microbiol. Mol. Biol. Rev. **66:**223–249.
12. **Davis, G. C., P. T. Kissinger, and R. E. Shoup.** 1981. Strategies for determination of serum or plasma norepinephrine by reverse-phase liquid chromatography. Anal. Chem. **53:**156–159.
13. **Dertz, E. A., J. Xu, A. Stintzi, and K. N. Raymond.** 2006. Bacillibactin-mediated iron transport in *Bacillus subtilis*. J. Am. Chem. Soc. **128:**22–23.
14. **Devireddy, L. R., C. Gazin, X. Zhu, and M. R. Green.** 2005. A cell-surface receptor for lipocalin 24p3 selectively mediates apoptosis and iron uptake. Cell **123:**1293–1305.
15. **Devireddy, L. R., J. G. Teodoro, F. A. Richard, and M. R. Green.** 2001. Induction of apoptosis by a secreted lipocalin that is transcriptionally regulated by IL-3 deprivation. Science **293:**829–834.
16. **Dowd, S. E.** 2007. *Escherichia coli* O157:H7 gene expression in the presence of catecholamine norepinephrine. FEMS Microbiol. Lett. **273:**214–223.
17. **Fischbach, M. A., H. Lin, D. R. Liu, and C. T. Walsh.** 2006. How pathogenic bacteria evade mammalian sabotage in the battle for iron. Nat. Chem. Biol. **2:**132–138.
18. **Fischbach, M. A., H. Lin, D. R. Liu, and C. T. Walsh.** 2005. *In vitro* characterization of IroB, a pathogen-associated *C*-glycosyltransferase. Proc. Natl. Acad. Sci. USA **102:**571–576.
19. **Fischbach, M. A., H. Lin, L. Zhou, Y. Yu, R. J. Abergel, D. R. Liu, K. N. Raymond, B. L. Wanner, R. K. Strong, C. T. Walsh, A. Aderem, and K. D. Smith.** 2006. The pathogen-associated *iroA* gene cluster mediates bacterial evasion of lipocalin 2. Proc. Natl. Acad. Sci. USA **103:**16502–16507.
20. **Flo, T. H., K. D. Smith, S. Sato, D. J. Rodriguez, M. A. Holmes, R. K. Strong, S. Akira, and A. Aderem.** 2004. Lipocalin 2 mediates an innate immune response to bacterial infection by sequestrating iron. Nature **432:**917–921.
21. **Fluckinger, M., H. Haas, P. Merschak, B. J. Glasgow, and B. Redl.** 2004. Human tear lipocalin exhibits antimicrobial activity by scavenging microbial siderophores. Antimicrob. Agents Chemother. **48:**3367–3372.
22. **Freestone, P. P., R. D. Haigh, P. H. Williams, and M. Lyte.** 2003. Involvement of enterobactin in norepinephrine-mediated iron supply from transferrin to enterohaemorrhagic *Escherichia coli*. FEMS Microbiol. Lett. **222:**39–43.
23. **Freestone, P. P., M. Lyte, C. P. Neal, A. F. Maggs, R. D. Haigh, and P. H. Williams.** 2000. The mammalian neuroendocrine hormone norepinephrine supplies iron for bacterial growth in the presence of transferrin or lactoferrin. J. Bacteriol. **182:**6091–6098.

24. **Freestone, P. P., P. H. Williams, R. D. Haigh, A. F. Maggs, C. P. Neal, and M. Lyte.** 2002. Growth stimulation of intestinal commensal *Escherichia coli* by catecholamines: a possible contributory factor in trauma-induced sepsis. Shock **18:**465–470.
25. **Goetz, D. H., M. A. Holmes, N. Borregaard, M. E. Bluhm, K. N. Raymond, and R. K. Strong.** 2002. The neutrophil lipocalin NGAL is a bacteriostatic agent that interferes with siderophore-mediated iron acquisition. Mol. Cell **10:**1033–1043.
26. **Hantke, K., G. Nicholson, W. Rabsch, and G. Winkelmann.** 2003. Salmochelins, siderophores of *Salmonella enterica* and uropathogenic *Escherichia coli* strains, are recognized by the outer membrane receptor IroN. Proc. Natl. Acad. Sci. USA **100:**3677–3682.
27. **Hoette, T. M., R. J. Abergel, J. Xu, R. K. Strong, and K. N. Raymond.** 2008. The role of electrostatics in siderophore recognition by the immunoprotein siderocalin. J. Am. Chem. Soc. **130:**17584–17592.
28. **Holmes, M. A., W. Paulsene, X. Jide, C. Ratledge, and R. K. Strong.** 2005. Siderocalin (Lcn 2) also binds carboxymycobactins, potentially defending against mycobacterial infections through iron sequestration. Structure **13:**29–41.
29. **Hvidberg, V., C. Jacobsen, R. K. Strong, J. B. Cowland, S. K. Moestrup, and N. Borregaard.** 2005. The endocytic receptor megalin binds the iron transporting neutrophil-gelatinase-associated lipocalin with high affinity and mediates its cellular uptake. FEBS Lett. **579:**773–777.
30. **Iannetti, A., F. Pacifico, R. Acquaviva, A. Lavorgna, E. Crescenzi, C. Vascotto, G. Tell, A. M. Salzano, A. Scaloni, E. Vuttariello, G. Chiappetta, S. Formisano, and A. Leonardi.** 2008. The neutrophil gelatinase-associated lipocalin (NGAL), a NF-κB-regulated gene, is a survival factor for thyroid neoplastic cells. Proc. Natl. Acad. Sci. USA **105:**14058–14063.
31. **Jewett, S. L., S. Eggling, and L. Geller.** 1997. Novel method to examine the formation of unstable 2:1 and 3:1 complexes of catecholamines and iron(III). J. Inorg. Biochem. **66:**165–173.
32. **Kerkut, G. A.** 1973. Catecholamines in invertebrates. Br. Med. Bull. **29:**100–103.
33. **Kulma, A., and J. Szopa.** 2007. Catecholamines are active compounds in plants. Plant Science **172:**433–440.
34. **Linert, W., E. Herlinger, R. F. Jameson, E. Kienzl, K. Jellinger, and M. B. Youdim.** 1996. Dopamine, 6-hydroxydopamine, iron, and dioxygen—their mutual interactions and possible implication in the development of Parkinson's disease. Biochim. Biophys. Acta **1316:**160–168.
35. **Loomis, L. D., and K. N. Raymond.** 1991. Solution equilibria of enterobactin and metal-enterobactin complexes. Inorg. Chem. **30:**906–911.
36. **Martin, R. B., J. Savory, S. Brown, R. L. Bertholf, and M. R. Wills.** 1987. Transferrin binding of Al^{3+} and Fe^{3+}. Clin. Chem. **33:**405–407.
37. **May, J. J., T. M. Wendrich, and M. A. Marahiel.** 2001. The *dhb* operon of *Bacillus subtilis* encodes the biosynthetic template for the catecholic siderophore 2,3-dihydroxybenzoate-glycine-threonine trimeric ester bacillibactin. J. Biol. Chem. **276:**7209–7217.
38. **McPherson, A.** 1999. Crystallization of biological macromolecules. Cold Spring Harbor Laboratory Press, Cold Spring Harbor, NY.
39. **Miethke, M., O. Klotz, U. Linne, J. J. May, C. L. Beckering, and M. A. Marahiel.** 2006. Ferri-bacillibactin uptake and hydrolysis in *Bacillus subtilis*. Mol. Microbiol. **61:**1413–1427.
40. **Miethke, M., and M. A. Marahiel.** 2007. Siderophore-based iron acquisition and pathogen control. Microbiol. Mol. Biol. Rev. **71:**413–451.
41. **Mori, K., H. T. Lee, D. Rapoport, I. R. Drexler, K. Foster, J. Yang, K. M. Schmidt-Ott, X. Chen, J. Y. Li, S. Weiss, J. Mishra, F. H. Cheema, G. Markowitz, T. Suganami, K. Sawai, M. Mukoyama, C. Kunis, V. D'Agati, P. Devarajan, and J. Barasch.** 2005. Endocytic delivery of lipocalin-siderophore-iron complex rescues the kidney from ischemia-reperfusion injury. J. Clin. Investig. **115:**610–621.
42. **Nakano, M., A. Takahashi, Y. Sakai, M. Kawano, N. Harada, K. Mawatari, and Y. Nakaya.** 2007. Catecholamine-induced stimulation of growth in *Vibrio* species. Lett. Appl. Microbiol. **44:**649–653.
43. **Newton, S. M., J. D. Igo, D. C. Scott, and P. E. Klebba.** 1999. Effect of loop deletions on the binding and transport of ferric enterobactin by FepA. Mol. Microbiol. **32:**1153–1165.
44. **Nurchi, V. M., T. Pivetta, J. I. Lachowicz, and G. Crisponi.** 2009. Effect of substituents on complex stability aimed at designing new iron(III) and aluminum(III) chelators. J. Inorg. Biochem. **103:**227–236.
45. **O'Donnell, P. M., H. Aviles, M. Lyte, and G. Sonnenfeld.** 2006. Enhancement of *in vitro* growth of pathogenic bacteria by norepinephrine: importance of inoculum density and role of transferrin. Appl. Environ. Microbiol. **72:**5097–5099.
46. **Ollinger, J., K. B. Song, H. Antelmann, M. Hecker, and J. D. Helmann.** 2006. Role of the Fur regulon in iron transport in *Bacillus subtilis*. J. Bacteriol. **188:**3664–3673.
47. **Raymond, K. N., and C. J. Carrano.** 1979. Coordination chemistry and microbial iron transport. J. Am. Chem. Soc. **12:**183–190.
48. **Russell, R. M.** 1992. Nutritional assessment, p. 1151–1155. *In* J. B. Wyngaarden, L. H. Smith, Jr., and J. C. Bennett (ed.), Cecil textbook of medicine, 19th ed. W. B. Saunders Co., Philadelphia, PA.
49. **Sambrook, J., and D. W. Russel.** 2001. Molecular cloning: a laboratory manual, 3rd ed. Cold Spring Harbor Laboratory Press, Cold Spring Harbor, NY.
50. **Schaible, U. E., and S. H. Kaufmann.** 2004. Iron and microbial infection. Nat. Rev. Microbiol. **2:**946–953.
51. **Schmidt-Ott, K. M., K. Mori, A. Kalandadze, J. Y. Li, N. Paragas, T. Nicholas, P. Devarajan, and J. Barasch.** 2006. Neutrophil gelatinase-associated lipocalin-mediated iron traffic in kidney epithelia. Curr. Opin. Nephrol. Hypertens. **15:**442–449.
52. **Sprencel, C., Z. Cao, Z. Qi, D. C. Scott, M. A. Montague, N. Ivanoff, J. Xu, K. M. Raymond, S. M. Newton, and P. E. Klebba.** 2000. Binding of ferric enterobactin by the *Escherichia coli* periplasmic protein FepB. J. Bacteriol. **182:**5359–5364.
53. **Studier, F. W., and B. A. Moffatt.** 1986. Use of bacteriophage T7 RNA polymerase to direct selective high-level expression of cloned genes. J. Mol. Biol. **189:**113–130.
54. **Stülke, J., R. Hanschke, and M. Hecker.** 1993. Temporal activation of β-glucanase synthesis in *Bacillus subtilis* is mediated by the GTP pool. J. Gen. Microbiol. **139:**2041–2045.
55. **Troadec, J. D., M. Marien, F. Darios, A. Hartmann, M. Ruberg, F. Colpaert, and P. P. Michel.** 2001. Noradrenaline provides long-term protection to dopaminergic neurons by reducing oxidative stress. J. Neurochem. **79:**200–210.
56. **Vlisidou, I., M. Lyte, P. M. van Diemen, P. Hawes, P. Monaghan, T. S. Wallis, and M. P. Stevens.** 2004. The neuroendocrine stress hormone norepinephrine augments *Escherichia coli* O157:H7-induced enteritis and adherence in a bovine ligated ileal loop model of infection. Infect. Immun. **72:**5446–5451.
57. **Vogt, M., and A. Skerra.** 2001. Bacterially produced apolipoprotein D binds progesterone and arachidonic acid, but not bilirubin or *E*-3M2H. J. Mol. Recognit. **14:**79–86.
58. **von Euler, U.** 1961. Occurence of catecholamines in acrania and invertebrates. Nature **190:**170.
59. **Vopel, S., H. Mühlbach, and A. Skerra.** 2005. Rational engineering of a fluorescein-binding anticalin for improved ligand affinity. Biol. Chem. **386:**1097–1104.
60. **Williams, P. H., W. Rabsch, U. Methner, W. Voigt, H. Tschape, and R. Reissbrodt.** 2006. Catecholate receptor proteins in *Salmonella enterica*: role in virulence and implications for vaccine development. Vaccine **24:**3840–3844.
61. **Yang, J., K. Mori, J. Y. Li, and J. Barasch.** 2003. Iron, lipocalin, and kidney epithelia. Am. J. Physiol. Renal Physiol. **285:**F9–F18.
62. **Zawadzka, A. M., R. J. Abergel, R. Nichiporuk, U. N. Andersen, and K. N. Raymond.** 2009. Siderophore-mediated iron acquisition systems in *Bacillus cereus*: identification of receptors for anthrax virulence-associated petrobactin. Biochemistry **48:**3645–3657.
63. **Zhu, M., M. Valdebenito, G. Winkelmann, and K. Hantke.** 2005. Functions of the siderophore esterases IroD and IroE in iron-salmochelin utilization. Microbiology **151:**2363–2372.